Monthly Notices
of the
ROYAL ASTRONOMICAL SOCIETY

MNRAS **480,** 4754–4760 (2018)
Advance Access publication 2018 August 13

doi:10.1093/mnras/sty2194

Calculated oscillator strengths for the strongest lines of cosmochronological interest in the visible spectrum of singly ionized uranium (U II)

S. Gamrath,[1] P. Palmeri[1] and P. Quinet[1,2]★

[1]*Physique Atomique et Astrophysique, Université de Mons, B-7000 Mons, Belgium*
[2]*IPNAS, Université de Liège, Sart Tilman, B-4000 Liège, Belgium*

Accepted 2018 August 8. Received 2018 August 03; in original form 2018 May 4

ABSTRACT

This work reports new calculations of radiative parameters for spectral lines of cosmochronological interest in singly ionized uranium. More precisely, a pseudo-relativistic Hartree-Fock model including core-polarization effects has been employed to compute the oscillator strengths corresponding to the strongest U II transitions in the visible wavelength range. The results obtained in the present investigation appear to be in reasonable agreement with the most accurate experimental data, reducing in that way the large scattering observed between the formerly published *gf* values. This allowed us to provide a list of 38 lines that could be used by astrophysicists as cosmochronometers in future studies to determine stellar ages from uranium radioactive decay.

Key words: atomic data – atomic processes.

1 INTRODUCTION

Oscillator strengths for radiative transitions in singly ionized uranium are of paramount importance in astrophysics, in particular in cosmochronology. It is indeed well known that the use of a long-lived radioisotope can be used to estimate the age of a star. Up until a few years ago, ^{232}Th, with a half-life of 14 Gyr, was used to date galactic stars (Butcher 1987, François et al. 1993, Cowan et al. 1999) but this radioisotope decays by approximately twice the lifetime of the Universe, and, as pointed out by Goriely & Clerbaux (1999), new accurate observations of heavy radioactive elements would be necessary to improve the accuracy of cosmochronometry analyses. More particularly, ^{238}U, with a half-life of 4.5 Gyr, represents a much more precise age indicator. Furthermore, the ratio U/Th might be a better cosmochronometer than either previously used Th/Eu or Th/Dy ratios, because of the much smaller mass difference between thorium and uranium than between either one of these two elements and the lighter lanthanides.

However, uranium is very hard to detect in stars. In 2001, Cayrel et al. (2001a) reported the first observation of a spectral line at a wavelength of 3859.57 Å, from singly ionized uranium, in the very metal-poor star BPS CS31082-001. This star, also called Cayrel's star, was found to be more metal deficient than the globular clusters, and was likely born in the Galaxy during very early times. This measurement, carried out with the high-resolution UVES spectrograph of the ESO/VLT telescope, gave rise to the determination of the age of formation of U and Th in the early Galaxy, using, for the first time, the U/Th ratio. The derived uranium abundance yielded an age 12.5 ± 3 Gyr, which led to the best estimate of the age of the Galaxy and consequently provided a lower limit to the age of the Universe. However, as mentioned by Cayrel et al. (2001b), the accuracy of this uranium dating is still affected by uncertainties in the measured abundance ratio, and in the calculated U/Th production ratio. The improvement of this situation depends not only on a better estimation of the production ratio U/Th, on advances in nuclear astrophysics models and on the investigation of other stars in which U and Th can be detected, but also on a comprehensive knowledge of the radiative properties for the potentially observable spectral lines, notably for the strongest U II electric dipole transitions.

To our knowledge, there have been very few available calculations of radiative parameters for singly ionized uranium so far. The main reason is that the complexity of the strongly mixed states involved in the lowest configurations, with five electrons distributed on the 5f, 6d, 7s, and 7p subshells, and the fragmentary knowledge of the experimental spectrum of this ion made theoretical computations extremely difficult. Most of the available oscillator strengths were deduced from quite old line intensities measured on arc spectra (Meggers, Corliss & Schribner 1961, Corliss & Bozman 1962, Voigt 1975, Corliss 1976, Kurucz 1995) if we except the results published by Nilsson et al. (2002) who obtained accurate *gf* values by combining branching fraction measurements with laboratory lifetimes determined using laser spectroscopy (Lundberg et al. 2001). These latter data concern however only a small number of strong U II lines.

★ E-mail: Pascal.QUINET@umons.ac.be

This lack of reliable radiative parameters in singly ionized uranium justifies the work reported in this paper. An additional motivation was also found in the new analysis of the experimental spectrum recently published for this ion by Meftah et al. (2017). More precisely, we carried out detailed calculations of oscillator strengths for the strongest U II transitions using the pseudo-relativistic Hartree-Fock (HFR) method (Cowan 1981) with core-polarization corrections (HFR+CPOL; Quinet et al. 1999, 2002, Quinet 2017). This allowed us to draw up a list of 38 visible spectral lines that could be used in cosmochronology.

2 AVAILABLE ATOMIC DATA IN U II

In their critical compilation related to actinides, Blaise & Wyart (1992) listed some preliminary U II energy levels, using the emission lines listed by Steinhaus et al. (1971) and Palmer, Keller & Engleman (1980), thus updating the previous estimates published by Brewer (1971). An uranium hollow-cathode Fourier transform spectrum between 1800 and 42 000cm^{-1} was then combined with previous visible and ultraviolet spectra by Blaise et al. (1994) who were able to determine the numerical values for 354 and 809 energy levels belonging to the four odd configurations 5f^{3}7s^2, 5f^{3}6d7s, 5f^{3}6d^2, 5f^{4}7p, and to the six even configurations 5f^{4}7s, 5f^{4}6d, 5f^{2}6d^{2}7s, 5f^{2}6d7s^2, 5f^{3}7s7p, 5f^{3}6d7p, respectively.

More recently, Meftah et al. (2017) used a parametric approach based on the Cowan (1981) codes to classify the lowest energy levels in singly ionized uranium. This work led to the identification of 253 levels belonging to the odd-parity configurations 5f^{3}7s^2 + 5f^{3}6d7s + 5f^{3}6d^2 + 5f^{4}7p + 5f^5, using 24 adjustable and 64 constrained radial parameters, with a root mean square (rms) deviation of 60 cm^{-1}. In the even parity, 125 levels were classified using a multiconfiguration basis including 5f^{4}7s + 5f^{4}6d + 5f^{2}6d^{2}7s + 5f^{2}6d7s^2 + 5f^{2}6d^3 by 22 free parameters with an rms deviation of 84 cm^{-1}. Moreover, a separate semi-empirical model, including only the higher even configurations 5f^{3}7s7p and 5f^{3}6d7p, led to the tentative classification of 12 energy levels within these configurations. Unfortunately, for these two configurations, the semi-empirical parametric fitting has to be limited to the adjustment of average energies and spin-orbit ζ_{5f} integrals, the quantitative evaluation of configuration interaction effects within the whole group 5f^4(7s + 6d) + 5f^2(6d + 7s)^3 + 5f^{3}7s7p + 5f^{3}6d7p having been tried unsuccesfully. Finally, the parametric study of Meftah et al. (2017) allowed them to re-investigate the high resolution ultraviolet spectrum of uranium recorded about 30 yr earlier at the Meudon Observatory. This led to the classification of 451 additional U II lines in the wavelength region 2344–2955 Å and the identification of one new level belonging to the 5f^{3}6d7p configuration.

As regards the radiative decay rates, the first measurements of relative line intensities in U II were obtained from emission arc spectra by Meggers et al. (1961), Corliss and Bozman (1962), Voigt (1975), and Corliss (1976). In the atlas of uranium lines published by Palmer et al. (1980), relative intensities were listed for 4928 U I and 431 U II emission spectral lines between 11 000 and 26 000cm^{-1}. The oscillator strengths of the lines at λ = 3859.571 Å and λ = 4050.041 Å were later determined by Chen & Borzileri (1981) who combined experimental lifetime measurements of the upper levels with unpublished branching fractions. Oscillator strengths were also reported for about 100 U II lines by Henrion, Fabry & Remy (1987) from relative intensities measured on a hollow-cathode lamp spectrum. In his data base, Kurucz (1995) listed oscillator strengths and transition probabilities for many U II lines based on the experimental data reported by Meggers et al. (1961), Corliss (1976), and Chen and Borzileri (1981). Finally, about 20 yr ago, accurate radiative lifetimes were measured by Lundberg et al. (2001), using laser-induced fluorescence technique, for six even-parity energy levels of singly ionized uranium located at 23 315.090cm^{-1} (J = 9/2), 24 684.132cm^{-1} (J = 9/2), 25 714.049cm^{-1} (J = 13/2), 26 191.309cm^{-1} (J = 13/2), 28 154.450cm^{-1} (J = 11/2), and 30 341.675cm^{-1} (J = 15/2). Experimental oscillator strengths for 57 U II lines in the region 3500–6700 Å were then determined by combining these latter radiative lifetimes with new branching fractions deduced from line intensity measurements performed using Fourier transform spectroscopy (Nilsson et al. 2002).

3 OSCILLATOR STRENGTH CALCULATIONS

Reliable atomic structure calculations in U II must take intravalence, core–valence, and core–core correlations into account, in addition to relativistic effects. In our work, we used the pseudo-relativistic HFR method (Cowan, 1981), in which the largest part of the intravalence correlation is represented by explicitly including a set of electronic configurations in the physical model, while the effects of core-excited configurations are modelled by a CPOL potential. As described e.g. by Quinet et al. (1999, 2002) and Quinet (2017) for atomic systems with n valence electrons, the one-particle operator of this potential can be written as

$$V_{P1} = -\frac{1}{2}\alpha_{\rm d}\sum_{i=1}^{n}\frac{r_i^2}{(r_i^2+r_{\rm c}^2)^3}, \quad (1)$$

where $\alpha_{\rm d}$ is the dipole polarizability of the ionic core and $r_{\rm c}$ is a suitable cut-off radius which is arbitrarily chosen as a measure of the size of the ionic core.

In addition, the interaction between the modified electric fields experienced by the valence electrons gives rise to a two-particle contribution given by

$$V_{P2} = -\alpha_{\rm d}\sum_{i>j}\frac{\vec{r}_i.\vec{r}_j}{\left[\left(r_i^2+r_{\rm c}^2\right)\left(r_j^2+r_{\rm c}^2\right)\right]^{3/2}}. \quad (2)$$

For consistency, in this HFR+CPOL method, the transition radial integral $\langle P_{nl}|r|P_{n'l'}\rangle$ has also to be replaced by

$$\left\langle P_{nl}|r\left(1-\frac{\alpha_{\rm d}}{\left(r^2+r_{\rm c}^2\right)^{3/2}}\right)|P_{n'l'}\right\rangle. \quad (3)$$

Moreover, in order to allow for a more accurate treatment of the penetration of the core by the valence electrons, a further correction has been included in our model. This correction, originally introduced by Hameed, Herzenberg & James (1968) and Hameed (1972), consists in the addition of the core-penetration term

$$\frac{1}{r_{\rm c}^3}\int_0^{r_{\rm c}} P_{nl}(r)r\,P_{n'l'}(r){\rm d}r. \quad (4)$$

to the integral

$$\left\langle P_{nl}(r)|\frac{r}{\left(r^2+r_{\rm c}^2\right)^{3/2}}|P_{n'l'}(r)\right\rangle \quad (5)$$

appearing in equations (2) and (3).

In this study, the configurations retained in the calculations were those presented by Meftah et al. (2017) as being the most interacting ones in the lowest part of the energy level spectrum, namely 5f^{3}7s^2, 5f^{3}6d7s, 5f^{3}6d^2, 5f^{4}7p, 5f^5 for the odd parity, and 5f^{4}7s, 5f^{4}6d, 5f^{2}6d^{2}7s, 5f^{2}6d7s^2, 5f^{2}6d^3, 5f^{3}7s7p, 5f^{3}6d7p for the even parity. This represents a total of 3237 and 6039 energy levels in each parity, respectively.

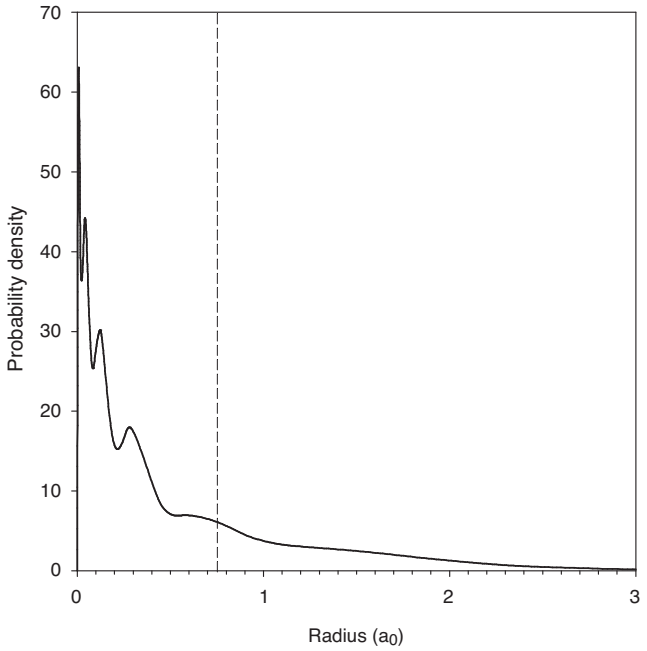

Figure 1. Electron probability density ($\sum P_{nl}^2$) of the ionic core in the ground configuration ($5f^3 7s^2$) of U II. The value of the cut-off radius used in the HFR+CPOL calculations ($r_c = 0.75$ a_0) is also shown in the figure. It represents the distance at which the electron probability density falls to 10 per cent of its maximum value, as suggested by Hameed (1972).

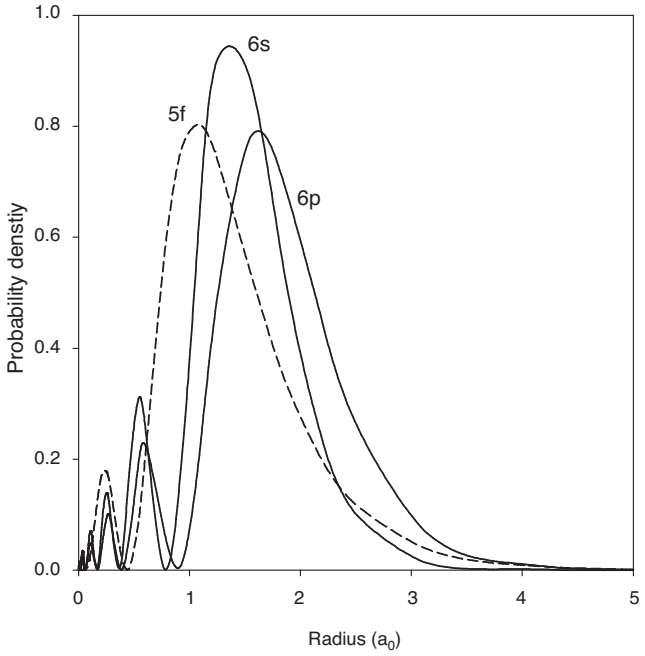

Figure 2. Electron probability densities (P_{nl}^2) of the outermost ionic core orbitals in U II, showing the collapse of 5f into the closed $6s^2 6p^6$ subshells.

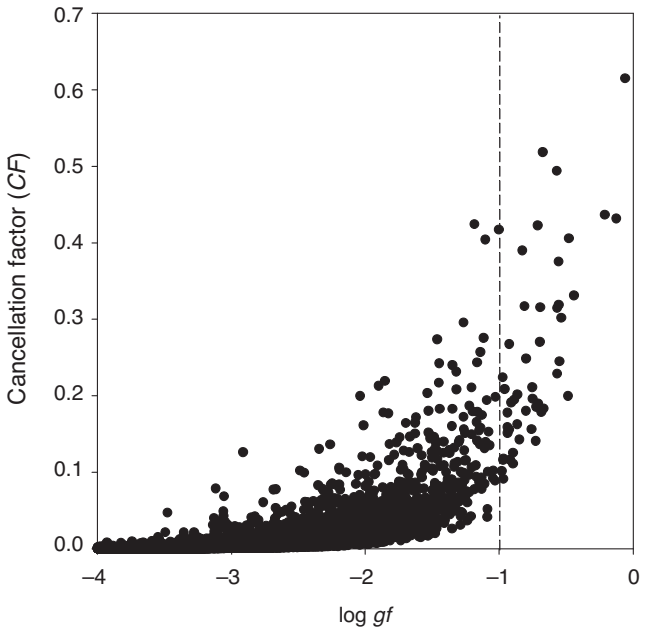

Figure 3. Cancellation factors plotted as a function of log *gf* values as obtained in this work for U II spectral lines. CF values smaller than typically 0.05 indicate that the corresponding *f* values may be affected by large percentage errors. Strong U II transitions with log $gf > -1$ do not appear to be affected by cancellation effects.

Since the configurations mentioned hereabove explicitly include a part of the correlation out of the $5f^2$ ionic core, CPOL effects were considered using the dipole polarizability, α_d, equal to 9.79 a_0^3 as tabulated by Fraga, Karwowski & Saxena (1976) for the U V ion. However, as mentioned, for example, by Hibbert (1982), the cut-off radius, r_c is not unambiguously defined. In this work, we used $r_c = 0.75$ a_0 which represents the distance at which the total probability density of the ionic core orbitals falls to 10 per cent of its maximum value, as suggested by Hameed (1972). Fig. 1 shows the calculated probability density of the core in the ground configuration $5f^3 7s^2$, together with the r_c value used in the computations. We noticed that, when using these α_d and r_c CPOL parameters, all the $\langle 6d|r|7p\rangle$ and $\langle 7s|r|7p\rangle$ electric dipole transition radial integrals were reduced by 20–25 per cent. However, for the singly ionized uranium, the analytical CPOL correction to the dipole operator introduced in equation (3) is no longer valid for transitions involving 5f electrons, the latter being deeply imbedded inside the closed $6s^2 6p^6$ subshells, as shown in Fig. 2. Instead, in order to take polarization effects into account for the 5f–6d transitions, the uncorrected $\langle 5f|r|6d\rangle$ radial integrals were scaled down by the factor 0.80, in a similar way to that used for computing the 4f–5d transitions in lowly ionized lanthanides (see e.g. Biémont et al. 2001; Li et al. 2001; Zhang et al. 2001; Biémont, Quinet & Ryabchikova 2002).

Finally, in order to reduce as much as possible the differences between calculated and available experimental energy levels, the fitted radial parameters reported by Meftah et al. (2017) were adopted for the five odd- and the seven even-parity configurations included in our physical model. As a reminder, for the odd configurations, Meftah et al. were able to fit up to 253 experimental energy levels with a final rms deviation of 60 cm^{-1} using 22 free and 64 constrained parameters among the average energies (E_{av}), the monoconfiguration and configuration interaction (CI) electrostatic integrals (F^k, G^k, R^k), the spin-orbit parameters (ζ_{nl}), the effective interaction operators (α, β, γ) and Slater forbidden parameters within the whole group of configurations $5f^3 7s^2 + 5f^3 6d7s + 5f^3 6d^2 + 5f^4 7p + 5f^5$. The semi-empirical fitting procedure was a little less satisfactory in the even parity, Meftah et al. (2017) being forced to separate their parametric analysis into two groups of configurations, i.e. $5f^4 7s +$

Table 1. Strongest visible spectral lines in U II. The transitions listed are limited to those for which the log *gf* values, computed in this work, are greater than −1.0.

λ^a_{air}	Lower odd level[b]		Upper even level[b]		log *gf*					
(Å)	E (cm^{-1})	J	E (cm^{-1})	J	C[c]	CB[d]	H[e]	K[f]	N[g]	This work[h]
3337.785	289.041	11/2	30 240.416	11/2	−1.28	–	–	−0.897	–	[−0.794]
3357.930	289.041	11/2	30 060.727	11/2	−1.39	–	–	−1.071	–	−0.703
3372.004	289.041	11/2	29 936.466	11/2	−1.46	–	–	−1.170	–	−0.351
3406.269	914.765	9/2	30 263.978	9/2	−1.42	–	–	−1.116	–	−0.892
3496.414	1749.123	13/2	30 341.673	15/2	−1.12	–	–	−0.691	−0.821	−0.595
3546.677	1749.123	13/2	29 936.466	11/2	−1.37	–	–	−1.066	−0.785	−0.549
3623.057	914.765	9/2	28 507.894	11/2	−1.29	–	–	−1.002	–	[−0.925]
3640.945	1749.123	13/2	29 206.703	11/2	−1.38	–	–	−1.121	–	−0.887
3670.068	914.765	9/2	28 154.447	11/2	−0.72	–	–	−0.173	−0.192	−0.556
3700.571	914.765	9/2	27929.924	11/2	−1.21	–	–	−0.904	–	−0.909
3724.983	1749.123	13/2	28 587.261	11/2	−1.45	–	–	−1.003	–	−0.896
3782.841	289.041	11/2	26 716.697	13/2	−0.89	–	–	−0.478	–	−0.674
3826.507	289.041	11/2	26 415.115	13/2	−1.17	–	−1.125	−0.904	–	−0.569
3859.571	289.041	11/2	26 191.312	13/2	−0.62	−0.204	−0.721	−0.105	−0.067	−0.058
3865.916	2294.696	11/2	28 154.447	11/2	−0.77	–	–	−0.273	−0.421	−0.800
3881.454	4585.434	13/2	30 341.673	15/2	−0.80	–	–	−0.279	−0.509	−0.465
3932.021	289.041	11/2	25 714.049	13/2	−0.89	–	−0.824	−0.528	−0.317	−0.478
3944.130	4585.434	13/2	29 932.395	15/2	−1.23	–	–	−0.928	–	−0.959
3985.793	5259.653	15/2	30 341.673	15/2	−0.71	–	–	−0.165	−0.278	−0.307
3990.420	914.765	9/2	25 967.697	7/2	−1.29	–	−1.745	−1.116	–	−0.925
4004.064	1749.123	13/2	26 716.697	13/2	−1.31	–	–	−1.138	–	−0.936
4044.412	5259.653	15/2	29 978.143	13/2	−0.97	–	–	−0.554	−0.706	−0.810
4051.912	5259.653	15/2	29 932.395	15/2	−0.95	–	–	−0.541	–	−0.692
4053.020	1749.123	13/2	26 415.115	13/2	−1.51	–	–	−1.448	–	−0.752
4090.133	1749.123	13/2	26 191.312	13/2	−0.78	–	–	−0.377	−0.184	−0.125
4116.097	0.000	9/2	24 288.004	11/2	−1.19	–	−1.194	−1.036	–	−0.712
4155.409	6283.431	13/2	30 341.673	15/2	−1.10	–	–	−0.759	−0.606	−0.948
4171.589	1749.123	13/2	25 714.049	13/2	−0.92	–	–	−0.606	−0.474	−0.567
4172.973	6283.431	13/2	30 240.416	11/2	−1.29	–	–	−1.051	–	[−0.917]
4174.189	5526.750	13/2	29 476.743	13/2	−1.21	–	–	−0.948	–	−0.865
4178.995	4585.434	13/2	28 507.894	11/2	−1.41	–	–	−1.261	–	[−0.667]
4211.658	4585.434	13/2	28 322.361	11/2	−1.25	–	–	−1.040	−0.811	−0.709
4241.664	4585.434	13/2	28 154.447	11/2	−0.83	–	–	−0.431	−0.103	−0.566
4282.460	4585.434	13/2	27 929.924	11/2	−1.37	–	–	−1.242	–	−0.684
4341.686	289.041	11/2	23 315.092	9/2	−1.24	–	−1.337	−1.161	−0.700	−0.536
4472.330	289.041	11/2	22 642.478	9/2	−1.28	–	−1.398	−1.260	–	−0.863
4555.091	8394.362	15/2	30 341.673	15/2	−1.34	–	–	−1.167	−0.650	−0.771
4627.075	4585.434	13/2	26 191.312	13/2	−1.27	–	–	−1.178	−0.593	−0.486

Notes. [a]Experimental wavelengths from Kurucz (1995).
[b]Experimental energy levels from Blaise et al. (1994) and Meftah et al. (2017).
[c]Values from Corliss (1976).
[d]Values from Chen and Borzileri (1981).
[e]Values from Henrion et al. (1987).
[f]Values from Kurucz (1995).
[g]Values from Nilsson et al. (2002).
[h]Values between square brackets correspond to uncertain line identifications in the calculations (see text).

$5f^46d + 5f^26d^27s + 5f^26d7s^2 + 5f^26d^3$, on the one hand, and $5f^37s7p + 5f^36d7p$, on the other hand. For the first group, an rms deviation of 84 cm^{-1} was found for 125 energy levels fitted with 22 radial parameters of the same type as those used in the odd parity. However, the interpretation of energy level structure of the second group with the same parametric method could only be carried out by adjusting only the average energies E_{av} and spin-orbit ζ_{5f} integrals, leading to an rms deviation of 441 cm^{-1} for 12 energy levels. In our work, when gathering all these seven even configurations together in the same model with the fitted parameters taken from Meftah el al. (2017), we found a rather good average energy deviation of 280 cm^{-1} for the levels of interest, i.e. those involved in the strongest transitions reported in Section 4.

4 RESULTS AND DISCUSSION

In view of their potential future use in cosmochronological studies, only the strongest spectral lines in singly ionized uranium were considered in this work. More precisely we limited our investigation to the electric dipole transitions for which the HFR+CPOL log *gf* values were found to be larger than −1. It was moreover noticed that most of the weaker transitions, i.e. with log $gf < -1$, were affected by cancellation effects. As a reminder, in order to calculate the oscillator strength for a transition between the atomic states βJ and $\beta' J'$, the line strength has to be computed

$$S = |\langle \beta J || P^{(1)} || \beta' J' \rangle|^2 \quad (6)$$

Table 2. Main *LS* coupling components of energy levels involved in the transitions listed in Table 1.

E (cm^{-1})[a]	J	1st component (per cent)	2nd component (per cent)	3rd component (per cent)
Odd parity				
0.000	9/2	77.0 5f^{3}7s^2 (^{4}I)^{4}I	12.6 5f^{3}7s^2 (^{2}H)^{2}H	3.6 5f^{3}6d^2 (^{4}I)^{4}I
289.041	11/2	76.8 5f^{3}6d7s (^{4}I)^{6}L	12.9 5f^{3}6d7s (^{2}H)^{4}K	4.9 5f^{3}6d7s (^{4}I)^{4}K
914.765	9/2	71.3 5f^{3}6d7s (^{4}I)^{6}K	10.5 5f^{3}6d7s (^{2}H)^{4}I	10.2 5f^{3}6d7s (^{4}I)^{4}I
1749.123	13/2	44.5 5f^{3}6d7s (^{4}I)^{6}L	26.1 5f^{3}6d7s (^{4}I)^{4}L	8.3 5f^{3}6d7s (^{2}H)^{4}K
2294.696	11/2	48.3 5f^{3}6d7s (^{4}I)^{6}K	17.6 5f^{3}6d7s (^{4}I)^{4}K	7.8 5f^{3}6d7s (^{4}I)^{4}I
4585.434	13/2	28.2 5f^{3}6d^2 (^{4}I)^{6}M	27.3 5f^{3}6d7s (^{4}I)^{6}L	14.3 5f^{3}6d7s (^{4}I)^{4}L
5259.653	15/2	67.5 5f^{3}6d7s (^{4}I)^{6}L	17.8 5f^{3}6d7s (^{4}I)^{4}L	6.4 5f^{3}6d7s (^{2}H)^{4}K
5526.750	13/2	71.0 5f^{3}6d7s (^{4}I)^{6}K	12.3 5f^{3}6d7s (^{4}I)^{4}K	5.5 5f^{3}6d7s (^{2}H)^{4}I
6283.431	13/2	38.4 5f^{3}6d^2 (^{4}I)^{6}M	21.6 5f^{3}6d7s (^{4}I)^{4}L	16.3 5f^{3}6d7s (^{4}I)^{6}L
8394.362	15/2	60.4 5f^{3}6d7s (^{4}I)^{6}K	14.2 5f^{3}6d^2 (^{4}I)^{6}M	4.8 5f^{3}6d7s (^{4}I)^{4}K
Even parity				
22642.478	9/2	10.4 5f^{3}7s7p (^{4}I)^{6}K	4.8 5f^{2}6d^{2}7s (^{3}F)^{4}I	3.9 5f^{2}6d^{2}7s (^{3}H)^{4}I
23315.092	9/2	23.7 5f^{3}7s7p (^{4}I)^{6}K	6.0 5f^{4}6d (^{5}I)^{6}G	5.0 5f^{3}7s7p (^{4}I)^{4}I
24288.004	11/2	7.9 5f^{3}7s7p (^{4}I)^{6}K	5.5 5f^{3}7s7p (^{4}I)^{4}K	3.6 5f^{4}6d (^{5}I)^{6}G
25714.049	13/2	9.1 5f^{3}6d7p (^{4}I)^{6}M	4.5 5f^{2}6d^{2}7s (^{3}H)^{4}K	4.0 5f^{2}6d^{2}7s (^{3}H)^{4}L
25967.697	7/2	19.7 5f^{3}7s7p (^{4}I)^{6}I	5.3 5f^{2}6d7s^2 (^{3}F)^{4}H	3.7 5f^{3}7s7p (^{4}I)^{4}H
26191.312	13/2	21.7 5f^{3}6d7p (^{4}I)^{6}M	8.9 5f^{2}6d^{2}7s (^{3}H)^{4}K	8.0 5f^{3}6d7p (^{4}I)^{4}L
26415.115	13/2	8.1 5f^{2}6d^{2}7s (^{3}H)^{6}H	7.1 5f^{3}6d7p (^{4}I)^{6}M	5.5 5f^{2}6d^{2}7s (^{3}H)^{4}K
26716.697	13/2	7.2 5f^{4}6d (^{5}F)^{6}H	5.6 5f^{2}6d^{2}7s (^{3}H)^{4}K	5.3 5f^{2}6d^{2}7s (^{1}G)^{4}K
27929.924	11/2	5.6 5f^{2}6d7s^2 (^{3}H)^{4}H	5.3 5f^{3}7s7p (^{4}I)^{6}K	4.5 5f^{3}6d7p (^{4}I)^{6}L
28154.447	11/2	7.0 5f^{3}6d7p (^{4}I)^{6}L	6.5 5f^{4}7s (^{3}H)^{4}H	3.5 5f^{4}7s (^{3}H)^{2}H
28322.361	11/2	8.1 5f^{3}6d7p (^{4}I)^{6}L	4.7 5f^{2}6d^{2}7s (^{3}F)^{6}H	3.6 5f^{2}6d^{2}7s (^{1}G)^{4}K
28507.894	11/2	5.0 5f^{4}6d (^{5}G)^{6}I	4.0 5f^{4}7s (^{3}H)^{4}H	3.7 5f^{2}6d7s^2 (^{3}H)^{4}H
28587.261	11/2	7.3 5f^{3}6d7p (^{4}I)^{6}L	5.3 5f^{2}6d^{2}7s (^{3}F)^{6}H	3.6 5f^{4}7s (^{1}H)^{2}H
29206.703	11/2	6.6 5f^{2}6d^3 (^{3}H)^{6}K	3.1 5f^{2}6d^3 (^{3}H)^{4}I	2.6 5f^{2}6d^{2}7s (^{3}F)^{6}G
29476.743	13/2	12.4 5f^{3}7s7p (^{4}I)^{6}K	5.1 5f^{2}6d^{2}7s (^{3}H)^{6}I	2.9 5f^{3}7s7p (^{4}I)^{4}K
29932.395	15/2	9.7 5f^{2}6d7s^2 (^{3}H)^{4}I	5.1 5f^{4}6d (^{5}F)^{6}H	5.0 5f^{3}6d7p (^{4}I)^{6}M
29936.466	11/2	11.9 5f^{3}6d7p (^{4}I)^{6}L	7.6 5f^{2}6d^{2}7s (^{3}F)^{6}G	4.7 5f^{2}6d^{2}7s (^{3}H)^{4}G
29978.143	13/2	13.9 5f^{2}6d^3 (^{3}H)^{6}K	5.1 5f^{2}6d^{2}7s (^{3}H)^{6}I	3.7 5f^{3}7s7p (^{4}I)^{6}K
30060.727	11/2	5.0 5f^{3}6d7p (^{4}I)^{6}L	4.4 5f^{2}6d^{2}7s (^{3}H)^{6}G	2.7 5f^{4}6d (^{5}F)^{4}G
30240.416	11/2	3.0 5f^{4}7s (^{3}H)^{2}H	2.8 5f^{3}6d7p (^{4}I)^{6}L	2.2 5f^{2}6d7s^2 (^{3}H)^{4}H
30263.978	9/2	11.6 5f^{3}7s7p (^{4}I)^{6}I	3.4 5f^{2}6d^3 (^{3}H)^{6}I	3.4 5f^{3}6d7p (^{4}I)^{6}K
30341.673	15/2	18.4 5f^{3}6d7p (^{4}I)^{6}M	12.4 5f^{4}7s (^{1}K)^{2}K	5.2 5f^{2}6d^{2}7s (^{3}H)^{2}L

Note. [a]Experimental energy levels from Blaise et al. (1994) and Meftah et al. (2017).

or its square root

$$S^{1/2} = \langle \beta J || P^{(1)} || \beta' J' \rangle, \tag{7}$$

where $P^{(1)}$ corresponds to the electric dipole operator. The wavefunctions are expanded in terms of basis functions due to intermediate coupling and configuration interaction mixing:

$$|\beta J > = \sum_{\gamma} y^{\beta}_{\gamma J} |\gamma J > \tag{8}$$

$$|\beta' J' > = \sum_{\gamma'} y^{\beta'}_{\gamma' J'} |\gamma' J' > \tag{9}$$

We may then write (7) in the form

$$S^{1/2} = \sum_{\gamma} \sum_{\gamma'} y^{\beta}_{\gamma J} \langle \gamma J || P^{(1)} || \gamma' J' \rangle y^{\beta'}_{\gamma' J'}. \tag{10}$$

This sum represents a mixing of amplitudes that frequently leads to destructive interference effects, in particular for weak lines. In making numerical calculations from (10), it is thus worthwhile evaluating a cancellation factor

$$\mathrm{CF} = \left[\frac{|\sum_{\gamma} \sum_{\gamma'} y^{\beta}_{\gamma J} < \gamma J || P^{(1)} || \gamma' J' > y^{\beta'}_{\gamma' J'}|}{\sum_{\gamma} \sum_{\gamma'} |y^{\beta}_{\gamma J} < \gamma J || P^{(1)} || \gamma' J' > y^{\beta'}_{\gamma' J'}|} \right]^2. \tag{11}$$

According to Cowan (1981), very small CF values (typically smaller than about 0.05) indicate that the corresponding line strengths may be expected to show large uncertainties. In Fig. 3, cancellation factors are plotted as a function of log gf for all U II transitions. We can clearly note that most of lines with log $gf < -1$ are affected by very small CF values indicating that the corresponding oscillator strengths could be unreliable. On the contrary, stronger transitions, with log $gf > -1$, do not appear to be affected by cancellation effects.

Such strong transitions, involving energy levels up to 30 342cm^{-1}, are reported in Table 1. This corresponds to 38 U II spectral lines appearing in the wavelength range from 3337 and 4627 Å. For these lines, our log gf values are compared with the 'old' data deduced from emission line intensity measurements by Corliss (1976), Chen and Borzileri (1981), Henrion et al. (1987) and Kurucz (1995), as well as with the more recent and more accurate experimental values obtained by Nilsson et al. (2002). It can be observed, from Table 1, that our calculated oscillator strengths are in reasonable agreement with the latter measurements, the mean relative difference between both sets of gf values being found to be equal to 25 per cent if we except four lines at 3670.068, 3865.916, 4155.409, and 4241.664 Å, for which our HFR+CPOL results are about a factor of 2 smaller than the experimental oscillator strengths of Nilsson et a (2002). It is worth noting however that, three of these

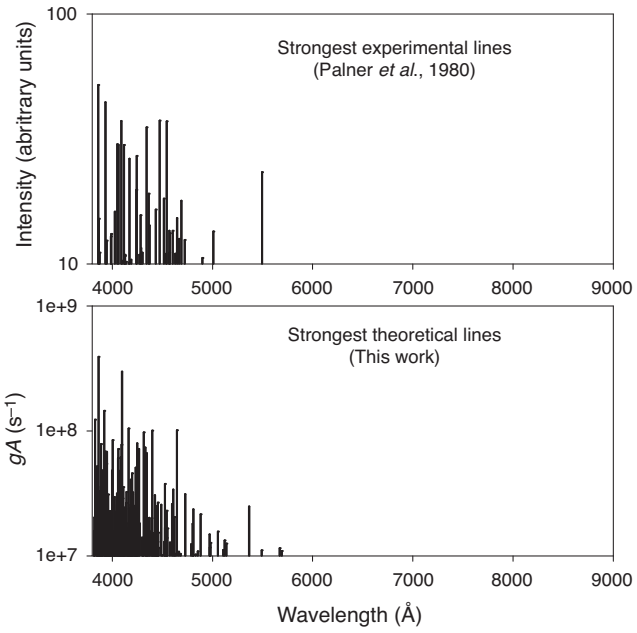

Figure 4. Comparison between experimental and theoretical strongest emission lines in U II. Only visible spectral lines observed by Palmer et al. (1980) with measured intensities greater than 10 (top figure) and those calculated in this work with weighted transition probabilities, gA, larger than 10^7 s^{-1} (bottom figure) are shown.

transitions are characterized by the same upper even-parity level at 28 154.451cm^{-1}, which was found to be extremely mixed, and thus very sensitive to small changes in the eigenvector composition. Indeed, for this level, our calculations led to a main *LS* component, i.e. 5f^3(^{4}I)6d7p ^{6}L$_{11/2}$, as weak as 7 per cent, to be compared with 18 per cent obtained by Meftah et al. (2017) using a much more limited physical model.

For four other spectral lines, at λ = 3337.785, 3623.057, 4172.973, and 4178.995 Å, our computed log gf values are given between square brackets in Table 1 to indicate that the corresponding results are likely to be affected by larger uncertainties. This is due to the fact that, for the two upper even-parity levels involved in these transitions, it was extremely difficult to establish a trustworthy correspondence between the experimental values, i.e. E = 28 507.894 and 30 240.416cm^{-1}, and the calculated ones, the retained theoretical levels being moreover very strongly mixed, with main *LS* components not exceeding 5 per cent, according to our calculations. These two levels were by the way not classified in the recent parametric analysis of the U II spectrum by Meftah et al. (2017).

The strength of intermediate coupling and configuration interaction characterizing the U II energy level structure is illustrated in Table 2 where the first three *LS* components, as calculated in this work, are given for all the levels involved in the transitions listed in Table 1. It is clear that the majority of levels appear to be extremely mixed, preventing any reliable spectroscopic designation. This is particularly the case for the even parity in which many levels were found to be the mixture of numerous significant contributions (sometimes up to 20) of comparable amplitudes.

A qualitative comparison between the strongest experimental and theoretical transitions is shown in Fig. 4, in which all the U II visible spectral lines observed by Palmer et al. (1980) with measured intensities greater than 10 are compared to those calculated in this work with weighted transition probabilities, gA, larger than 10^7 s^{-1}. It is clearly seen that the overall agreement between both spectra is very satisfactory.

It is also particularly interesting to consider the line at 3859.571 Å, which was used as cosmochronometer by Cayrel et al. (2001a). For this line, our gf value of 0.875 is in excellent agreement with the accurate experimental result reported by Nilsson et al. (2002), i.e. gf = 0.857, whereas all the previous data were very scattered between gf values so different as 0.240 (Corliss 1976), 0.625 (Chen and Borzileri 1981), 0.190 (Henrion et al. 1987), and 0.785 (Kurucz 1995).

Finally, it was found that CPOL effects considered in our physical model have a major influence on the final oscillator strengths, the mean ratio $gf_{\rm HFR+CPOL}/gf_{\rm HFR}$ being found to be equal to 0.57. These effects, which are assumed to take account of the most important core–valence and core–core correlations, are expected to be much larger than those of intravalence correlations not explicitly considered in our multiconfiguration expansions. It was indeed verified that our computed transition rates were slightly sensitive to additional valence configurations. More precisely, in a first step, the configurations 5f^{2}7s^{2}7p, 5f^{2}6d7s7p, 5f^{2}6d^{2}7p, 5f^{2}7s7p^2, and 5f^{2}6d7p^2 were investigated. By comparing a nine-configuration ab intio HFR calculation (including 5f^{3}7s^2, 5f^{3}6d7s, 5f^{3}6d^2, 5f^{4}7s, 5f^{4}6d, 5f^{2}6d7s^2, 5f^{2}6d^{2}7s, 5f^{3}7s7p, and 5f^{3}6d7p) with a fourteen-configuration calculation (adding 5f^{2}7s^{2}7p, 5f^{2}6d7s7p, 5f^{2}6d^{2}7p, 5f^{2}7s7p^2, and 5f^{2}6d7p^2) the effect of the latter five configurations was estimated and found rather small. Indeed, the mean difference for the strongest lines (log $gf > -1$) was 0.09 dex, which corresponds to a relative discrepancy of a few percent. When adding 5f^{3}7s7d, 5f^{3}6d7d, 5f^{4}7d, 5f^{2}7s^{2}7d, and 5f^{2}6d^{2}7d to the nine-configuration expansion, the mean difference was then 0.05 dex. Finally, the inclusion of the 5f^{3}7s8s, 5f^{3}6d8s, 5f^{4}8s, 5f^{2}6d^{2}8s, 5f^{2}7s^{2}8s, 5f^{3}7s8p, and 5f^{3}6d8p was found to affect the log gf values by less than 0.04 dex.

5 CONCLUSION

This work represents the first attempt to establish a reliable list of U II spectral lines that could be used in cosmochronology, corresponding to 38 strong electric dipole transitions in the wavelength visible region. To do so, a pseudo-relativistic HFR model including CPOL corrections was employed to compute the oscillator strengths, the latter being found in satisfactory overall agreement with the most accurate experimental data, where available. In view of the complexity of the U II spectrum, it is clear, however, that additional efforts, on both the experimental and theoretical sides, are still needed for improving the accuracy of the radiative parameters in this spectrum of high cosmochronological interest.

ACKNOWLEDGEMENTS

PP and PQ are, respectively, Research Associate and Research Director of the Belgian Fund for Scientific Research FRS-FNRS. Financial support from this organization is gratefully acknowledged.

REFERENCES

Biémont E. et al., 2001, MNRAS, 321, 481
Biémont E., Quinet P., Ryabchikova T. A., 2002, MNRAS, 336, 1155

Blaise J., Wyart J.-F., 1992, Selected Constants Energy Levels and Atomic Spectra of Actinides Vol. 22. Centre National de la Recherche Scientifique, Paris
Blaise J., Wyart J.-F., Vergés J., Engleman R., Jr, Palmer B. A., Radziemski L. J., 1994, J. Opt. Soc. Am. B, 11, 1897
Brewer L., 1971, J. Opt. Soc. Am., 12, 1666
Butcher H. R., 1987, Nature, 328, 127
Cayrel R. et al., 2001a, Nature, 409, 691
Cayrel R. et al., 2001b, in von Hippel T., Simpson C., Manset N., eds, ASP Conf. Ser., Vol. 245: Astrophysical Ages and Times Scales. Astron. Soc. Pac., San Francisco, p. 244
Chen H. L., Borzileri C., 1981, J. Chem. Phys., 74, 6063
Corliss C. H., 1976, J. Res. Natl. Bur. Stand., 80A, 429
Corliss C. H., Bozman W. R., 1962, NBS Monograph 53. US Government Printing Office, Washington DC
Cowan R. D., 1981, The Theory of Atomic Structure and Spectra. California Univ. Press, Berkeley
Cowan J. J., Pfeiffer B., Kratz K. L., Thielemann F. K., Sneden C., Burles S., Tytler D., Beers T. C., 1999, ApJ, 521, 194
Fraga S., Karwowski J., Saxena K. M. S., 1976 , Handbook of Atomic Data. Elsevier, Amsterdam
François P., Spite M., Spite F., 1993, A&A, 274, 821
Goriely S., Clerbaux B., 1999, A&A, 346, 798
Hameed S., 1972, J. Phys. B, 5, 746
Hameed S., Herzenberg A., James M. G., 1968, J. Phys. B, 1, 822
Henrion G., Fabry M., Remy M., 1987, J. Quant. Spectrosc. Radiat. Transfer., 37, 477
Hibbert A., 1982, Nucl. Instrum. Methods Phys. Res., 202, 323
Kurucz R. L., 1995, Atomic Spectral line Database from CD-ROM 23. Available online at https://www.cfa.harvard.edu/amp/ampdata/kurucz23/sekur.html (accessed in 2018 April)
Li Z. S. et al., 2001, J. Phys. B, 34, 1349
Lundberg H., Johansson S., Nilsson H., Zhang Z., 2001, A&A, 372, L50
Meftah A., Sabri M., Wyart J. F., Tchang-Brillet W. Ü., 2017, Atoms, 5, 24
Meggers W. F., Corliss C. H., Schribner B. F., 1961, NBS Monograph 32. US Government Printing Office, Washington DC
Nilsson H., Ivarsson S., Johansson S., Lundberg H., 2002, A&A, 381, 1090
Palmer B. A., Keller R. A., Engleman R.,, Jr , 1980, LASL Informal Report LA-8251-MS, UC-34a. Los Alamos Scientific Laboratory, NM, USA
Quinet P., 2017, Can. J. Phys., 95, 790
Quinet P., Palmeri P., Biémont E., McCurdy M. M., Rieger G., Pinnington E. H., Wickliffe M. E., Lawler J. E., 1999, MNRAS, 307, 934
Quinet P., Palmeri P., Biémont E., Li Z. S., Zhang Z. G., Svanberg S., 2002, J. Alloys Compd., 344, 255
Steinhaus D. W., Radziemski L. J.,, Jr, Cowan R. D., Blaise J., Guelachvili G., Ben Osman Z., Vergès J., 1971, LASL Report LA-4501, UC-34. Los Alamos Scientific Laboratory, NM, USA
Voigt P. A., 1975, Phys. Rev. A, 11, 1845
Zhang Z. G., Li Z. S., Svanberg S., Palmeri P., Quinet P., Biémont E., 2001, Eur. Phys. J. D, 15, 301

This paper has been typeset from a TEX/LATEX file prepared by the author.